

Satellite Remote Bathymetry: A New Mechanism for Modeling

Wei Ji¹, Daniel L. Civco, and William C. Kennard

Laboratory for Earth Resources Information Systems², Department of Natural Resources Management & Engineering, The University of Connecticut, Storrs, CT 06269-4087

ABSTRACT: A new mechanism for remote bathymetric modeling that overcomes inherent deficiencies of previous remote bathymetric techniques is presented. Spectral observations indicate that the emergent radiance from water is dominated by water column scattering rather than by the bottom reflection, unless the water is very shallow and transparent or overlies a highly reflecting bottom. Observation of this phenomenon has made it possible to develop a water column scattering-based remote bathymetric model which can be applied to turbid and somewhat deep coastal waters. Analysis of both satellite sensor (Landsat TM and SPOT-XS) and *in situ*-observed data indicates that this model can describe the relationship between the reflected radiance from water and water column depth better than the bottom reflection-based model. This paper also presents an approach to calculate the attenuation coefficient of water with *in situ* spectral measurements and to integrate the coefficient into the model calibration in order to eliminate atmospheric effects. In addition, a quantitative expression for the maximum detectable water depth is given using this water column scattering-based theory.

INTRODUCTION

THE NEED FOR MAPPING MARINE HAZARDS and for updating navigational charts in shallow waters has led many researchers to develop satellite remote bathymetric techniques. Among them, a group of scientists at the Environmental Research Institute of Michigan initiated investigations in this field in the late 1960s and have made major contributions to both principles and methods (Polcyn and Sattinger, 1969; Polcyn and Lyzenga, 1973; Polcyn and Lyzenga, 1979; Lyzenga, 1977; Lyzenga, 1978; Lyzenga, 1979; Lyzenga, 1981; Tanis and Hallada, 1984; Tanis and Byrne, 1985). They developed a bottom reflection-based remote bathymetric theory which can be expressed as follows for the single-band approach:

$$L_i = L_{i\infty} + L_0 R_b(\lambda) e^{-k_i f Z} \quad (1)$$

where L_i is the radiance value in band i , $L_{i\infty}$ is the average radiance over deep water due to the reflection from the water column and surface and scattering from the atmosphere; L_0 is a constant which is the product of the irradiance at the sea surface, the transmittance of the sea surface and atmosphere, and the reduction of the radiance due to refraction at the sea surface; $R_b(\lambda)$ is the bottom reflectance; k_i is the effective attenuation coefficient of the water; f is a geometric factor to account for path length through the column in a "round trip;" and Z is bottom depth. This model, which has been the basis of almost all remote bathymetric techniques to date, states that the sensor-recorded energy reflected from water bottom is inversely proportional to the depth of water after eliminating atmospheric and water column effects. It has been recognized that the following assumptions are an inherent part of the bottom reflection-based theory: a high bottom reflectance, an appropriate level of water quality, and/or a shallow depth. The bottom-reflected energy would be too weak to be sensed by the satellite sensor if these conditions were not met. This has greatly limited the application of remote bathymetric techniques in coastal waters that are turbid and have poorly reflecting bottoms, where predictions beyond a metre or two are required.

¹Presently with TGS Technology, Inc., U.S. Fish & Wildlife Service's National Wetlands Research Center Operations, 1010 Gause Blvd., Slidell, LA 70458.

²Formerly Laboratory for Remote Sensing.

With the bottom reflection-based model (Equation 1), atmospheric and water column effects are to be eliminated by deducting the average deep water radiance from the sensor signals (through $L_i - L_{i\infty}$). It is intended with this approach to provide theoretical completion for modeling and seems to be accepted without question about its validity. Examining this approach by our study, however, has revealed that it can introduce an error in model calculations due to applying a constant deduction to the locations having lower water column contribution (or "over deduction") and a zero (or even a negative) value of $L_i - L_{i\infty}$ can be anticipated in some cases.

These inherent deficiencies of earlier models make it difficult to apply remote bathymetric technique to most coastal waters and has slowed the development of new algorithms. A new theory which can provide a basis for effective remote bathymetry for most coastal waters, which are turbid and have weak-reflecting bottoms with a varied range of depth, becomes necessary.

RECONSIDERATION OF RADIATIVE MECHANISM OF REMOTE BATHYMETRY

There are many indications that the emergent radiance from water is dominated by scattering in the water column rather than by the bottom reflection unless the water depth is very shallow, the water is very clear, and/or there is a highly reflective bottom. In our study, *in situ*, satellite-synchronous observations were recorded for upwelling radiance and depth to bottom of shallow water over three major bottom types: sandy, muddy, and vegetation-covered (grassy). Table 1 shows that spectral reflectance measurements over sandy bottoms generally have

TABLE 1. LOG REFLECTANCE VERSUS WATER DEPTHS

λ (μm)	Bottom types	Sample size	r^2	Prob > F	Significance
0.45-0.52	sandy	15	0.38	0.0110	*
0.45-0.52	muddy	9	0.26	0.1339	
0.45-0.52	grassy	13	0.17	0.1371	
0.52-0.60	sandy	15	0.61	0.0003	**
0.52-0.60	muddy	9	0.04	0.5670	
0.52-0.60	grassy	13	0.001	0.9088	

* significant; ** highly significant.

an acceptable correlation with the water depth while this usually does not occur for those data measured over other types having low reflectance.

The data in Figure 1 also show that reflectance values, as determined with *in situ* radiometer measurements emulating TM band 1, from deeper areas are generally higher than those from shallower areas, contrary to the situation in very shallow areas, so that the reflectance curve looks somewhat like the shape of a saddle. The analysis of satellite sensor data using the bottom reflection-based model generally shows a low accuracy as anticipated (see the section entitled "Model Verification").

Such facts have generated a framework for developing a water column scattering-based theory for remote bathymetric modeling which is stated as follows:

"The back-scattered energy from coastal water is quantitatively related to the water column depth if the assumption of vertical homogeneity is valid. This relationship can be expressed with an appropriate radiative transfer model and can be associated with satellite sensor signals through a carefully designed algorithm of which atmospheric correction is a major function. With this theory, the bottom-reflected energy is ignored so that bottom conditions have only a negligible direct effect on upwelling radiation from the water. Instead, horizontal variations of upwelling radiance are caused by horizontal inhomogeneity of water mass which is, to some extent, related to suspension of bottom materials (note: with the bottom reflection-based theory, horizontal effects in remote bathymetry were directly related to variation of bottom reflectance over study areas)."

RADIATIVE TRANSFER MODEL

To express quantitatively the relationship stated by the water column scattering-based theory, an appropriate radiative transfer model is needed. For this purpose, the Singly Scattered Irradiance (SSI) Model developed by Philpot (1987, 1989) was adapted due to its advantage of separating optically deep and shallow water effects, as well as for its simplicity. A modification has been made by simply ignoring the bottom reflection, and a new version of SSI becomes

$$R(0-) = R_s [1 - \exp(-KZ)] \quad (2)$$

where $R(0-)$ is the irradiance reflectance just below the water surface and R_s is the irradiance reflectance of an optically deep water column. This equation can be transformed into a version

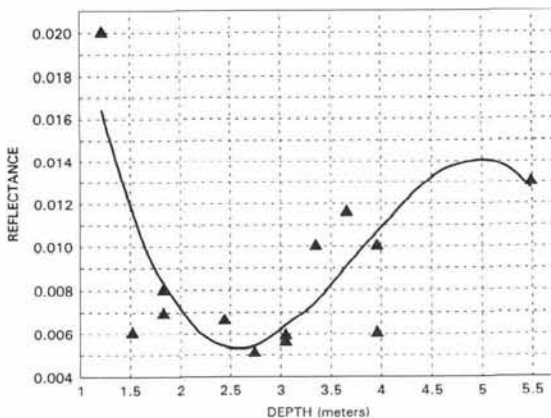


FIG. 1. Water reflectance at various depths as determined with coupled *in situ* radiometer and fathometer observations (data collected coincident with 13 May 1988 Landsat overpass).

describing the radiance sensed by the satellite remote sensor L_s by including some environmental factors:

$$L_s = C_0 T_a R_s [1 - \exp(-KZ)] + T_a \rho_a L_k + L_p \quad (3)$$

or

$$L_s = A[1 - \exp(-KZ)] + B \quad (4)$$

where

- C_0 = a factor relating to downwelling irradiance, Fresnel reflectance in water, and index of refraction of water;
- T_a = atmospheric transmission factor;
- ρ_a = Fresnel reflectance in air;
- L_k = sky irradiance; and
- L_p = path radiance.

Note that $A = C_0 T_a R_s$ and $B = T_a \rho_a L_k + L_p$ in Equation 4 can be treated as constants for a given scene.

With Equations 3 or 4, water column depth within certain ranges can be associated with the signal observed at satellite height, and the restrictions of the bottom reflection-based model have been overcome due to the new model's property of back-scattering dependence. If K , A , and B in Equation 4 can be estimated, then Equation 4 will become an operational model for determining water column depth with remotely sensed data. An algorithm has been developed to carry out this task.

ALGORITHM DESIGN

The algorithm is a two-step procedure. First, calculate K values from *in situ* spectral measurements using Equation 2 through ratioing technique. Next, with K values calculated and a group of values of L_s and Z , A and B in Equation 4 are estimated. With K , A , and B values, calculation of water column depths can be performed with the inversion of Equation 4.

CALCULATION OF K VALUES

Equation 2 is used to calculate K value with *in situ* measurements. For two spatially proximal locations, there are four measurements: $R(0-)_1$, $R(0-)_2$, Z_1 , and Z_2 , so that

$$R(0-)_1 = R_{s1} [1 - \exp(-K_1 Z_1)] \quad (5)$$

and

$$R(0-)_2 = R_{s2} [1 - \exp(-K_2 Z_2)] \quad (6)$$

A ratio of Equation 5 and Equation 6 results in

$$\frac{R(0-)_1}{R(0-)_2} = \frac{R_{s1} [1 - \exp(-K_1 Z_1)]}{R_{s2} [1 - \exp(-K_2 Z_2)]} \quad (7)$$

For the two proximal locations, one can assume a horizontal homogeneity of water quality; thus, $R_{s1} = R_{s2}$ and $K_1 = K_2 = K$. Therefore, Equation 7 is reduced to

$$\frac{R(0-)_1}{R(0-)_2} = \frac{[1 - \exp(-KZ_1)]}{[1 - \exp(-KZ_2)]} \quad (8)$$

Applying a power series expansion to approximate $\exp(-KZ)$, solve Equation 8 for K : i.e.,

$$\exp(-KZ) = 1 + \frac{(-KZ)}{1!} + \frac{(-KZ)^2}{2!} + \frac{(-KZ)^3}{3!} + \dots + \frac{(-KZ)^n}{n!} + \dots \quad (9)$$

In the visible region of the electromagnetic spectrum, and for typical coastal waters and appropriate Z values, the value of KZ is usually smaller than 1; therefore, $(-KZ)^n/n!$ for $n \geq 3$ will

have a very small value and can be ignored. Thus, an approximation is obtained for $\exp(-KZ)$: i.e.,

$$\exp(-KZ) = 1 + \frac{(-KZ)}{1!} + \frac{(-KZ)^2}{2!} \quad (10)$$

Substituting Equation 10 into Equation 8, we come to

$$\frac{R(0-)_{1}}{R(0-)_{2}} = \frac{1 - \left[1 + (-KZ_1) + \frac{1}{2}(-KZ_1)^2 \right]}{1 - \left[1 + (-KZ_2) + \frac{1}{2}(-KZ_2)^2 \right]} \quad (11)$$

Rearranging Equation 11, K is expressed with a compact form:

$$K = \frac{2R(0-)_{1}Z_2 - 2R(0-)_{2}Z_1}{R(0-)_{1}Z_2^2 - R(0-)_{2}Z_1^2} (m^{-1}) \quad (12)$$

In measurement of reflectance of sea water, a specially designed two-part enclosure was used to adapt a terrestrial, hand-held radiometer to measure upwelling radiance $R(-0)$ beneath the surface (Brown *et al.*, 1989). The basic function of the enclosure is to protect the radiometer from water while keeping measurements unaffected by surface reflection. The radiometer was immersed in the water to within a few centimetres of the surface when measurements were taken.

To calculate K values, the paired measurements, two values of $R(0-)$ and the corresponding depths, were chosen from those which were not only spatially proximal and with significant difference of depth, but also from depths as deep as possible and from a bottom of low reflectance such as muddy conditions to avoid possible minor bottom effects. Calculated K values using the above criteria were considered as representative of the corresponding data groups.

Table 2 lists K values for each scene with respect to the band pass and the bottom type, showing that K values generally increase with longer wavelengths (from TM band 1 to band 3) which is consistent with published *in situ* measurements (K values corresponding to the first three bands of TM and the first two bands of SPOT-XS were calculated).

PARAMETER ESTIMATION

Once K values have been obtained, the model parameters A and B in Equation 4 can be estimated using a transformed Equation 4 with sea truth depth data: i.e.,

$$L_s = AX + B \quad (13)$$

where $X = 1 - \exp(-KZ)$.

With A and B estimated, the operational model was derived by solving Equation 4 for Z : i.e.,

$$Z = -\frac{1}{K} \ln\left(1 - \frac{L_s - B}{A}\right) \quad (14)$$

Note that B contains only atmospheric and sky irradiance ef-

fects. Thus, the term $L_s - B$ accounts for these effects without "the over-deduction" problem with the bottom reflection-based model.

THE MODEL FOR VERY SHALLOW WATERS

As noted previously and also as shown by *in situ* measurements, when the water is very shallow (usually < 2 m) and/or particularly with a highly reflecting sandy bottom, the bottom-reflected energy could be dominant in emergent radiation from water. Such a situation has led to a solution to this "marginal effect" by adapting the bottom reflection-based model with a modification of the approach to eliminate the atmospheric effect. Philpot's SSI model is used again but with an elimination of the deep water effect; thus, we have

$$L_b = \hat{A} \exp(-KZ) + B \quad (15)$$

where $\hat{A} = T_a C_o R_b$. Solving Equation 15 for Z :

$$Z = -\frac{1}{K} \ln\left(\frac{L_b - B}{\hat{A}}\right) \quad (16)$$

Note that B in Equation 16, which is estimated with deep water data, is the same as B used in Equation 14. Equation 16 has the same form as One-Band Model (Equation 1).

MODEL VERIFICATION

Regression analyses were performed with Equation 14 using satellite sensor data and adequate sea data sets (water depth Z) to verify the water column scattering-based model and to estimate the parameters of the model, and with the same data sets a bottom reflection-based model was also tested for comparison. A statistical program was written to conduct these analyses. The term $X (= 1 - \exp(-KZ))$ was calculated with K and Z values for each observation and was used as an independent variable rather than depth Z , because X is simply a transformation of Z . The analyses were based on SPOT-XS data of 9 May 1988 and Landsat TM data of 13 March 1989. To test the effect of bottom reflection on the water column scattering-based model, analyses were also conducted successively with exclusion of observations corresponding to the depths in the order from the shallow to the deep. For example, all observations were used for the first analysis while the single observation corresponding to the depth less than or equal to 0.6 m was excluded for the second analysis, and several observations corresponding to the depth less than or equal to 0.9 m were deleted for the third analysis, and so on until an acceptable minimum number of observations was reached. Similarly, to test the effect of water depth on the significance of the bottom reflection-based model, analyses were conducted with exclusion of observations in the order from the deep to the shallow.

The analyses show that the largest correlation coefficients for the water column scattering-based model are 0.56 (P value = 0.0001) and 0.51 (P value = 0.0001) with TM band 1 and SPOT-XS band 1, respectively, indicating a highly significant model ($\alpha = 0.05$). In contrast, a small correlation exists for the bottom reflection-based model, with the highest correlation coefficients of 0.24 (P value = 0.0037) and 0.29 (P value = 0.0010) for TM band 2 and SPOT-XS band 1, respectively.

The above analyses also indicate for the water column scattering-based model that a higher correlation exists with the shorter wavelength band (blue band) because the correlation coefficients for TM bands 2 and 3 and SPOT-XS band 2 are 0.31 (P value = 0.0058), 0.29 (P value = 0.0079), and 0.13 (P value = 0.0320), respectively. Most likely, this is due to the penetrating peak in coastal waters being in the blue to the blue-green regions of the electromagnetic spectrum (the significantly different penetrating abilities of different bands raises a question about the mul-

TABLE 2. CALCULATED K (1/M) VALUES FOR EACH SCENE

SPOT-XS 9 May 1988	TM 13 May 1988	TM 20 Oct 1988	TM 13 Mar 1989
0.20	0.26	0.34	0.17
(XS 1, muddy)	(TM 1, grassy)	(TM 1, muddy)	(TM 1, muddy)
0.18	0.27	0.29	0.24
(XS 2, muddy)	(TM 2, grassy)	(TM 2, muddy)	(TM 2, muddy)
	0.47	0.37	0.31
	(TM 3, grassy)	(TM 3, muddy)	(TM 3, muddy)

tiband approach to satellite remote bathymetry because different bands provide information about waters at different depths). Also, due to the water penetrating ability, the model with TM band 1 (blue band) data tends to be affected by "shallow water effect" - the bottom reflection in contrast to the models with SPOT-XS band 1 (green band) and TM band 2 (green band) data. Thus, the best correlation for TM band 1 data was obtained after several observations, corresponding to depths less than 1.5 m, were excluded from the analyses.

The water column scattering-based bathymetric model (Equation 14) has been applied, using ERDAS* image processing system, to Landsat TM data of 13 March 1989 to calculate predicted water depths of the study area. Before the model calculation, the satellite sensor image was processed to mask out all land mass and islands with a technique developed for this study (Ji, 1991) so that only the water portion was processed for water depth prediction. The resulting depth map shows a significant coincidence with the bottom depth data on the nautical chart of the study area (National Ocean Service, NOAA, 1985). In several areas, such as the area near the entrance of Pawcatuck River and throughout Little Naragasset Bay, predicted depth values do not coincide well with the nautical chart. This may be caused by significant local variation of water quality or bottom conditions.

QUANTITATIVE ERROR SOURCES OF THE MODEL

Even though the model with the first band data of both Landsat TM and SPOT-XS was highly significant, moderate correlation coefficients suggest that notable quantitative errors still could be anticipated if the inversion of this calibrated model (Equation 14) were used to predict water depths. Major error sources might be as follows:

- The simplified radiative transfer theory might be too crude to describe precisely the radiative processes in water and the boundary of water-air.
- Possible spatial variations in environmental parameters within the scene make the assumptions of vertical and horizontal homogeneity, the mainstay of the remote bathymetric models, invalid.
- Unavoidable fluctuations in sea depth measurements.
- The sensor's ability is limited in water penetration and depth resolution.
- The data with transit depths from very shallow to deep may be subject to significant effects of both water column scattering and bottom reflection and might introduce quantitative errors when using a "scattering-based model."

THE MAXIMUM DETECTABLE DEPTH

In remote bathymetry, the maximum detectable depth is a function not only of wavelength, but also the sensor's dynamic range (maximum and minimum recorded radiance values) and the quantization level, which are all fixed and are available from sensor calibration data. The definition of the maximum detectable depth (Z_{max}) is the depth at which the difference between the observed radiance and that for an optically deep water mass is equivalent to the identifiable minimum radiance σ : i.e.,

$$L_z - L_{Z_{max}} = \sigma \quad (17)$$

with

$$\sigma = \frac{L_{max} - L_{min}}{N} \quad (18)$$

where L_{max} and L_{min} are recorded effective maximum and minimum radiance values for each band of the sensor, and N is the quantization level of the sensor which is 256 for both TM and

SPOT-XS. Substituting Equation 17 into Equation 4 and solving it for Z_{max} , we have an expression for Z_{max} for the scattering-based model:

$$Z_{max} = -\frac{1}{K} \ln\left(1 - \frac{\sigma - \beta}{A}\right) \quad (19)$$

or

$$Z_{max} = -\frac{1}{K} \ln\left(1 - \frac{L_{max} - L_{min} - (T_a \rho_a L_k + L_p) N}{C_0 T_a R_z N}\right) \quad (20)$$

Equation 20 shows how Z_{max} is determined by water quality, environmental parameters, and the sensor's characteristics. Inputting K , A , β , and σ values into Equation 19, the maximum detectable depths for TM bands 1, 2, and 3 were calculated to be 6.4, 3.0, and 2.1 metres, respectively. These values corresponded to water quality and atmospheric conditions of 13 March 1989. The validity of Equation 19 has been verified by the fact that 97 percent of the predicted water depth values with the water column scattering-based model for TM band 1 data of 13 March 1989 were less than 6.4 m.

CONCLUSIONS

- The bottom reflection-based model has been found to be valid usually only in very shallow waters, generally requiring a highly reflecting bottom and/or a high water transparency. Satellite sensor data analyses indicated that the procedure of deducting the average deep water radiance from the sensed radiances of shallower locations could introduce an error into the calculations. This was due to over-deduction between locations with different water column contributions. This situation, thus, restricts use of the bottom reflection-based model to coastal waters.
- Observations from both *in situ* and satellite measurements have revealed that back-scattering of the water column can dominate the upwelling irradiance, and bottom reflection usually is only a minor effect in those areas which are turbid, deep, and/or have weakly reflecting bottom coverages, a more common situation for applying remote bathymetric techniques. This fact has generated a framework to develop a new mechanism of remote bathymetric modeling.
- The remote bathymetric model based upon column scattering theory has succeeded in yielding a more precise description of the relationship between the sensed radiance and the water depth beyond very shallow areas. Statistical analyses with the column scattering-based model showed that correlation between satellite sensor radiance values and water depths was highly significant for both TM and SPOT-XS band 1, and was significant for TM bands 2 and 3. This was in contrast to the relatively small correlation obtained with bottom reflection-based model for the same data sets.
- Predicted water depths with the water column scattering-based model and TM band 1 data of 13 March 1989 showed a significant agreement with the sea data.
- The approach developed to calculate water attenuation coefficients with *in situ* spectral measurements has provided a way to integrate water quality, a very important factor, into bathymetric modeling so that the model can be calibrated more precisely.
- The maximum detectable depth in satellite remote bathymetry can be defined in terms of maximum and minimum sensed radiance values and the quantization level of the satellite sensor and can be formulated with the column scattering-based bathymetric model.

ACKNOWLEDGMENTS

This research was supported in part by NOAA Grant NA-85AA-D-SG101 as Project R/O E-1 of the Connecticut Sea Grant Program. This paper is submitted as Storrs Agricultural Experiment Station Contribution Number 1372.

REFERENCES

- Brown, C. W., D. L. Civco, and W. C. Kennard, 1989. Adaptation of a

*ERDAS is the product of Earth Resources Data Analysis Systems, Inc., Atlanta, Georgia.

Hand-Held Radiometer for Measuring Upwelling Radiance in the Aquatic Environment. *Photogrammetric Engineering & Remote Sensing*, Vol. 55, No. 2, pp. 193-194.

Ji, W., 1991. *Satellite Remote Bathymetry: A Study of Quantitative Models*. Ph.D. Dissertation. The University of Connecticut, Storrs, Connecticut.

Lyzenga, D. R., 1977. Reflectance of a Flat Ocean in the Limit of Zero Water Depth. *Applied Optics*, Vol. 16, No. 2, pp. 282-283.

——, 1978. Passive Remote Sensing Techniques for Mapping Water Depth and Bottom Features. *Applied Optics*, Vol. 17, No.3, pp. 379-383.

——, 1979. Shallow Water Reflectance Modeling with Applications to Remote Sensing of Ocean Floor, *Proceedings of 13th International Symposium on Remote Sensing of Environment*, Ann Arbor, Michigan. pp. 583-602.

——, 1981. Remote Sensing of Bottom Reflectance and Water Attenuation Parameters in Shallow Water Using Aircraft and Landsat Data. *International Journal of Remote Sensing*, Vol. 2, No. 1, pp. 71-82.

Philpot, W. D., 1987. Radiative Transfer in Stratified Waters: A Single-Scattering Approximation for Irradiance. *Applied Optics*, Vol. 26, No. 19, pp. 4123-4132.

——, 1989. Bathymetric Mapping with Passive Multispectral Imagery. *Applied Optics*, Vol. 28, No. 8, pp. 1569-1578.

Polcyn, F. C., and I. J. Sattinger, 1969. Water Depth Determination Using Remote Sensing Techniques. *Proceedings of 6th International Symposium on Remote Sensing of Environment*, Ann Arbor, Michigan. pp. 1017-1028.

Polcyn, F. C., and D. R. Lyzenga, 1973. Calculation of Water Depth from ERTS-MSS Data. *Proceedings Symposium on Significant Results Obtained from ERTS-1*, New Carrollton, Maryland. pp. 1433-1436.

——, 1979. Landsat Bathymetry Mapping by Multitemporal Processing. *Proceedings of 13th International Symposium on Remote Sensing of Environment*, Ann Arbor, Michigan. pp. 1269-1276.

Tanis, F. J., and W. A. Hallada, 1984. Evaluation of Landsat Thematic Mapper Data for Shallow Water Bathymetry. *Proceedings of 18th International Symposium on Remote Sensing of Environment*, Ann Arbor, Michigan. pp. 629-643.

Tanis, F. J., and H. J. Byrne, 1985. Optimization of Multispectral Sensors for Bathymetry Applications. *Proceedings of 19th International Symposium on Remote Sensing of Environment*. Ann Arbor, Michigan. pp. 865-874.

(Received 15 May 1991; accepted 21 August 1991)

DON'T MISS THE PREMIER CONFERENCE DEDICATED TO THE USE OF COMPUTERS IN

- Facilities Management
- Forestry
- Geodesy
- Geography
- Mapping
- Photogrammetry
- Remote Sensing
- Spatial Analysis



**Nov. 8-12, 1992
San Jose, California
San Jose Convention Center**

The GIS/LIS Conference and Exposition is sponsored by the American Congress on Surveying and Mapping (ACSM), the American Society for Photogrammetry and Remote Sensing (ASPRS), AM/FM International, the Association of American Geographers (AAG), and the Urban and Regional Information Systems Association (URISA)

For more information, complete and return this form to:

GIS/LIS '92
5410 Grosvenor Lane, Suite 100
Bethesda, Maryland 20814-2122

You may call 301- 493-0200, or send a fax to 301- 493-8245.

Name _____

Address _____

City _____ State _____ Zip _____

Country _____

Include membership information for:

- AAG ACSM ASPRS AM/FM International URISA